Free-energy landscape for a tagged particle in a dense hard-sphere fluid

Takashi Yoshidome,* Takashi Odagaki, and Akira Yoshimori
Department of Physics, Kyushu University, Fukuoka 812-8581, Japan
(Received 2 September 2007; published 3 June 2008)

Exploiting the thermodynamic potential functional provided by density functional theory, we determine analytically the free-energy landscape (FEL) in a hard-sphere fluid. The FEL is represented in the three-dimensional coordinate space of the tagged particle. We also analyze the distribution of the free-energy barrier between adjacent basins and show that the most provable value and the average of the free-energy barrier are increasing functions of the density. Since the size of the cooperatively rearranging region (CRR) is also increased as the density is raised [Yoshidome *et al.*, Phys. Rev. E **76**, 021506 (2007)], the present result is consistent with the Adam-Gibbs theory in which the increase of the activation energy is due to the increase of the size of the CRR.

DOI: 10.1103/PhysRevE.77.061503 PACS number(s): 64.70.P−

I. INTRODUCTION

Understanding the glass transition remains one of the most important unsolved problems in condensed matter physics. A principal concern is to develop a general framework which is capable of elucidating both the thermodynamic [1,2] and dynamic [3,4] characteristics near the glass transition temperature T_g. Although several attempts such as the mode-coupling theory [5], the replica method of the glass transition [6], and the potential-energy landscape approach [7–10] have been proposed, they lack the desired capability.

We have recently proposed the free-energy landscape (FEL) picture which provided a unified phenomenological understanding of the characteristics of the glass transition [11–14]. The FEL can be defined by the free energy calculated from the phase space around given $3N$ position coordinates $\{\mathbf{R}_i\}$ [12,14] ($\mathbf{R}_i$ is the position of the ith particle and N is the number of the particles in the system), and thus the FEL is a function of $\{\mathbf{R}_i\}$, temperature, and density. The FEL is expected to have many basins near T_g. Here, we refer to a basin as the region in which each configuration approaches the same minimum by steepest-descent minimization [8]. The structural relaxation corresponds to the transition from a basin to one of the adjacent basins. Several characteristics near T_g such as the self-diffusion [15–19], specific heat anomaly at the glass transition [20–24], aging [25,26], and behavior of the generalized susceptibility [14] have been explained qualitatively on the basis of the FEL picture.

Both thermodynamic and dynamic characteristics can be understood qualitatively by the FEL picture. In order to describe the glass transition quantitatively, it is necessary to construct the FEL from first principles and analyze the structure of the FEL. In this paper, we investigate the FEL for a hard-sphere fluid by exploiting the thermodynamic potential of density functional theory [11–13]. Since the structural relaxation is considered to be determined within a cooperatively rearranging region (CRR) [11–13], we concentrate on the FEL for a CRR. In particular, for the purpose of simplifying the presentation of the FEL, we put a tag on a given particle and force a displacement of the tagged particle in several directions. All other particles in the CRR are relaxed to a stable position. The FEL constructed by this procedure corresponds to a three-dimensional cut of the entire FEL. We analyze the statistics of the FEL at different densities through the distribution of the free-energy barrier between two basins. In order to obtain good statistics, we put a tag on all particles in the CRR in turn and find barriers.

We organize this paper as follows: We first present a method for the construction of the FEL in Sec. II. In Sec. III, the FEL for a tagged particle in a three-dimensional view is presented. We obtain the distribution function of the free-energy barrier between basins and its density dependence in Sec. IV. A summary and discussion are given in Sec. V.

II. FREE-ENERGY LANDSCAPE BY DENSITY FUNCTIONAL THEORY

A. Definition

We have proposed [11–13] that the FEL can be constructed using the thermodynamic potential functional of density functional theory [27,28] in which the grand potential $\Omega[\rho(\mathbf{r})]$ is expressed as a functional of the density field, $\rho(\mathbf{r})$. The grand potential can be expressed as a function of $\{\mathbf{R}_i\}$ using a sum of Gaussian functions for $\rho(\mathbf{r})$:

$$\rho_{\mathrm{Gauss}}(\mathbf{r}) = \left(\frac{\alpha}{\pi}\right)^{3/2} \sum_i \exp[-\alpha(\mathbf{r}-\mathbf{R}_i)^2]. \tag{1}$$

Here α and $\mathbf{R}_i$ are the degree of the spread of the density distribution and the average position of the ith particle, respectively. The density field (1) represents the distribution of the motion around $\{\mathbf{R}_i\}$ by the Gaussian functions and means that the motion within $|\mathbf{r}-\mathbf{R}_i| \leq 1/\sqrt{\alpha}$ is coarse grained by α. Using Eq. (1), $\Omega[\rho(\mathbf{r})]$ can be expressed as a function of α and $\{\mathbf{R}_i\}$:

$$\Omega(\alpha,\{\mathbf{R}_i\}) \equiv \Omega[\rho_{\mathrm{Gauss}}(\mathbf{r})]. \tag{2}$$

For a fixed value of α, this defines the FEL as a function of $\{\mathbf{R}_i\}$ [11–13].

*Present address: Institute of Advanced Energy, Kyoto University, Uji, Kyoto 611-0011, Japan. t-yoshidome@iae.kyoto-u.ac.jp

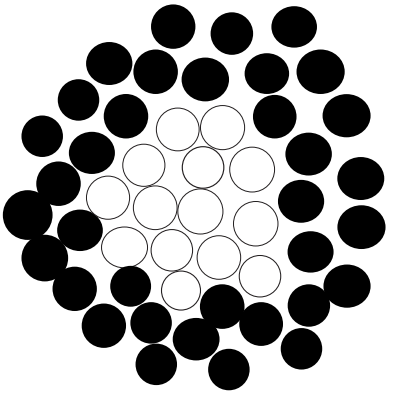

FIG. 1. A schematic representation of the model under consideration. The black particles are fixed, and the white particles form the CRR.

B. Ramakrishnan-Yussouff free-energy functional

We employ the free-energy functional developed by Ramakrishnan and Yussouff for $\Omega[\rho(\mathbf{r})]$ [29]. This free-energy functional has been used for the liquid-crystal transition [28,30] and the glass transition [31–39]. Ramakrishnan and Yussouff expressed $\Omega[\rho(\mathbf{r})]$ as follows [29]:

$$\beta\,\Delta\Omega[\rho(\mathbf{r})] \equiv \beta\Omega[\rho(\mathbf{r})] - \beta\Omega[\bar{\rho}] = \int_V d\mathbf{r}\,\rho(\mathbf{r})\ln\left[\frac{\rho(\mathbf{r})}{\bar{\rho}}\right] - \frac{1}{2}\int_V d\mathbf{r}_1\int_V d\mathbf{r}_2 \times c_2(|\mathbf{r}_1-\mathbf{r}_2|)[\rho(\mathbf{r}_1)-\bar{\rho}][\rho(\mathbf{r}_2)-\bar{\rho}], \quad (3)$$

where $\bar{\rho}$ is the uniform density defined by $\bar{\rho}\equiv\frac{1}{V}\int d\mathbf{r}\,\rho(\mathbf{r})$ and $c_2(|\mathbf{r}_1-\mathbf{r}_2|)$ is the direct correlation function at $\bar{\rho}$. In addition, $\beta=(k_BT)^{-1}$ where k_B is the Boltzmann constant and T is the absolute temperature. We use the Percus-Yevick approximation for the direct correlation function of the hard-sphere system [40]. Note that the essential point of the following results and discussions does not change if we employ other free-energy functionals such as the weighted density functional [41,42] and the free-energy functional of the fundamental measure theory [43]. We also note that α is treated as a constant in this paper for simplicity, though one may have to incorporate the temperature dependence of α for a quantitative analysis of the glass transition.

III. FREE-ENERGY LANDSCAPE FOR A TAGGED PARTICLE

We are interested in the FEL which is responsible for the structural relaxation caused by particles within the CRR [11–13]. In the previous paper [13], we estimated the size of the CRR in the following manner. Assuming that the shape of the CRR is a sphere (see Fig. 1), we first confine the particles in the spherical shell made by fixing the particles. In order to obtain the particle configuration $\{\mathbf{R}_i\}$ at the minimum in the basin, the particles in the confining area are relaxed to minimize $\Omega(\alpha,\{\mathbf{R}_i\})$ in $\{\mathbf{R}_i\}$ space. We then calculate the FEL for given positions of a selected particle. Other particles in the confined space are relaxed with the position of the selected particle fixed. If a transition to the adjacent basin occurs, we decrease the size of the confining area and calculate the FEL in the new confining area. By reducing the number of particles in the confined area further, one can find the critical number at which a transition to the adjacent basin cannot take place. This critical number is N_{CRR}. In the previous paper, we estimated that N_{CRR} is $8<N_{\mathrm{CRR}}<14$ at $\bar{\rho}\sigma^3=0.90$, $10<N_{\mathrm{CRR}}<18$ at $\bar{\rho}\sigma^3=0.963$, and $27<N_{\mathrm{CRR}}<32$ at $\bar{\rho}\sigma^3=1.06$. Here σ is the diameter of the hard sphere.

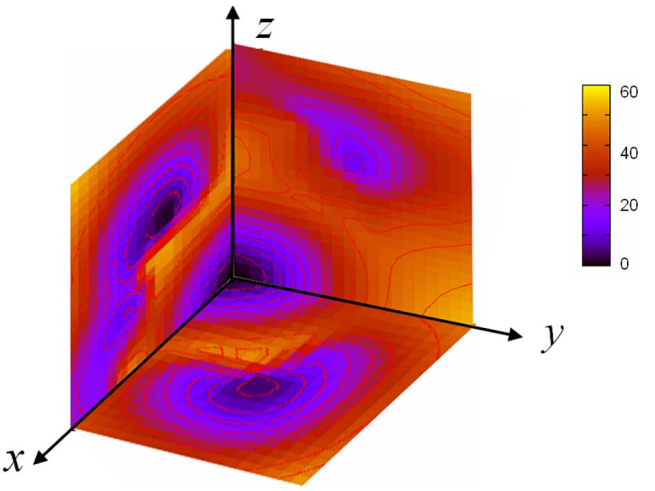

FIG. 2. (Color online) The FEL of a tagged particle for $\bar{\rho}\sigma^3=0.90$ on x-y, y-z, and z-x planes in the first quadrant. x, y, and z denote the displacement of the tagged particle. The parameter α is set to $\alpha\sigma^2=36$.

When we construct the FEL for a tagged particle, the particles are confined in a spherical shell made by fixed particles (see Fig. 1). The number of particles in the spherical shell is assumed to be the upper value of the size of the CRR at each density. We assume $\alpha\sigma^2=36$ [13], corresponding to the mean-squared displacement of the particle in a fcc structure at the melting point [30]. We then initialize the position of particles within the CRR by relaxing them to a minimum of the grand potential $\Omega(\alpha,\{\mathbf{R}_i\})$ in $\{\mathbf{R}_i\}$ space. The steepest-descent method is employed for the relaxation. In order to make the presentation simple, we calculate the FEL for a process in which a tagged particle near the center of the shell is forced to be displaced in several directions and the positions of the other particles are relaxed to minimize $\Omega(\alpha,\{\mathbf{R}_i\})$ in $\{\mathbf{R}_i\}$ space with the position of the tagged particle fixed. The FEL obtained here corresponds to a three-dimensional cut of the entire FEL.

Figure 2 shows the FEL for the tagged particle at $\bar{\rho}\sigma^3=0.90$ in the first quadrant. Here contours of the free energy are shown on the x-y, y-z, and z-x planes. The origin is the initial position of the tagged particle, and x, y, and z represent the displacement in each direction.

We also survey wider areas on the x-y, y-z, and z-x planes and construct a contour plot of the FEL. Figures 3(a)–3(c) show the contour plot of the FEL on these three planes. There are two basins on the y-z plane at $(y/\sigma,z/\sigma)=(0.8,1.2)$ and $(-0.4,1.4)$ in addition to the initial basin at the origin. These two basins are separated from the initial

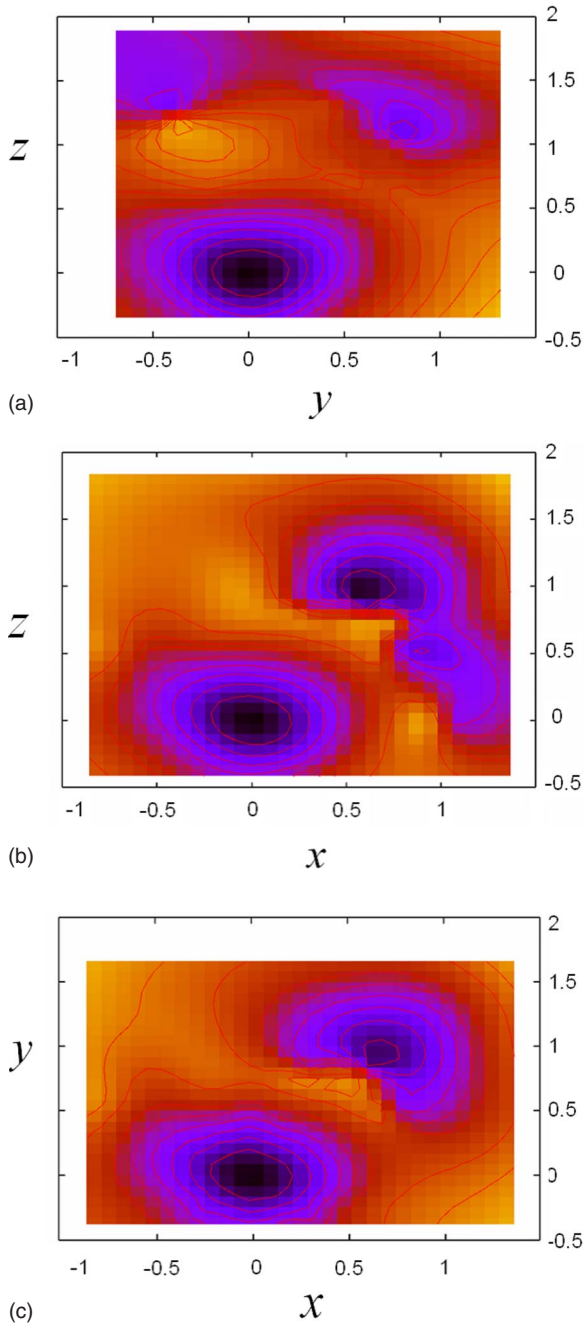

FIG. 3. (Color online) Contour plots of the FEL of the tagged particle on the (a) y-z, (b) z-x, and (c) x-y planes. $\bar{\rho}\sigma^3=0.90$ and $\alpha\sigma^2=36$. The initial basin is at the origin. The color scale is the same as the one shown in Fig. 2.

basin by a barrier of $(30-60)k_BT$. The height of the barrier between these two basins is approximately $40k_BT$.

On the x-z plane, there are two basins at $(x/\sigma, z/\sigma)=(0.6, 1.0)$ and $(0.9, 0.5)$ in addition to one at the origin. The barrier between these two basins and the initial basin is $(30-50)k_BT$, and the height of the barrier between them is approximately $20k_BT$.

On the x-y plane, one basin is presented at $(x/\sigma, y/\sigma)=(0.7, 0.95)$ in addition to one at the origin. The free-energy barrier between this basin and the basin at the origin is $(30-50)k_BT$. We observe the FEL on other planes and found similar structures.

IV. DISTRIBUTION OF THE BARRIERS

As shown in Figs. 2 and 3, the FEL consists of many basins and barriers. To obtain the statistics of the structure, we investigate the distribution of barriers between two adjacent basins. We displace the tagged particle in 26 isotropic directions selected from the lozenge dodecahedron surrounding the original position of the tagged particle: 12 directions perpendicular to the face of the dodecahedron and 14 directions to the vertices of the dodecahedron. Other particles in the confined area are relaxed with the position of the tagged particle fixed. We assume that the two particles do not overlap when $|\mathbf{R}_i-\mathbf{R}_j| \geq \sigma-\sigma/\sqrt{\alpha}$, since the positions of the particles are distributed around $\{\mathbf{R}_i\}$ with a width of $\sigma/\sqrt{\alpha}$ [13].

We define the transition state as follows [13]. Starting from the initial configuration $\{\mathbf{R}_i^{\text{initial}}\}$ which is at the minimum of an initial basin, we first obtain a configuration $\{\mathbf{R}_i\}$ from the calculation above. We then relax the configuration $\{\mathbf{R}_i\}$ to reach a minimum $\{\mathbf{R}_i^{\text{min}}\}$. This configuration $\{\mathbf{R}_i^{\text{min}}\}$ is compared with the initial configuration $\{\mathbf{R}_i^{\text{initial}}\}$. If $\{\mathbf{R}_i^{\text{min}}\}$ differs from $\{\mathbf{R}_i^{\text{initial}}\}$, the system can be considered to have passed a barrier between the basins and we regard the position just before the second basin as the transition state. The free-energy barrier ΔF is defined as the difference between the free energy at the transition state and that at the initial state. Although the barrier may not correspond to the saddle between two basins, the relative error is of the order of a few percent $(\sim 1/N_{\text{CRR}})$ [44], since all particles other than the tagged particle are fully relaxed in the process to reach the barrier. In order to obtain better statistics, we performed this procedure for all particles one by one, and thus we examined $26N_{\text{CRR}}$ paths in the FEL.

Figures 4(a)–4(c) show histograms of the free-energy barrier at three different densities, $\bar{\rho}\sigma^3=0.9$, 0.963, and 1.06. For $\bar{\rho}\sigma^3=0.9$ [Fig. 4(a)], the free-energy barrier is distributed between $18.75k_BT$ and $46.25k_BT$ and the distribution is asymmetric with respect to the maximum at $23.75k_BT$. Similar properties are also observed for densities $\bar{\rho}\sigma^3=0.963$ [Fig. 4(b)] and $\bar{\rho}\sigma^3=1.06$ [Fig. 4(c)].

We find that as the density is increased, the most provable value of the free-energy barrier (e.g., $23.75k_BT$ at $\bar{\rho}\sigma^3=0.9$) increases and the distribution of the free-energy barrier moves to a higher free-energy region.

In Fig. 5, we show the density dependence of the most provable value and the average of the free-energy barrier.

As shown in the previous paper [13], N_{CRR} is also an increasing function of the density. Our results are consistent with the Adam-Gibbs theory [45] in which the increase of the activation energy is due to an increase of N_{CRR}. In fact, Fig. 6 shows that the ratio $\beta\Delta F/N_{\text{CRR}}$ does not depend much on the density. Here the most probable value is used for $\beta\Delta F$.

V. SUMMARY AND DISCUSSION

In this paper, we have demonstrated that the FEL for disordered systems and its statistics can be obtained analytically

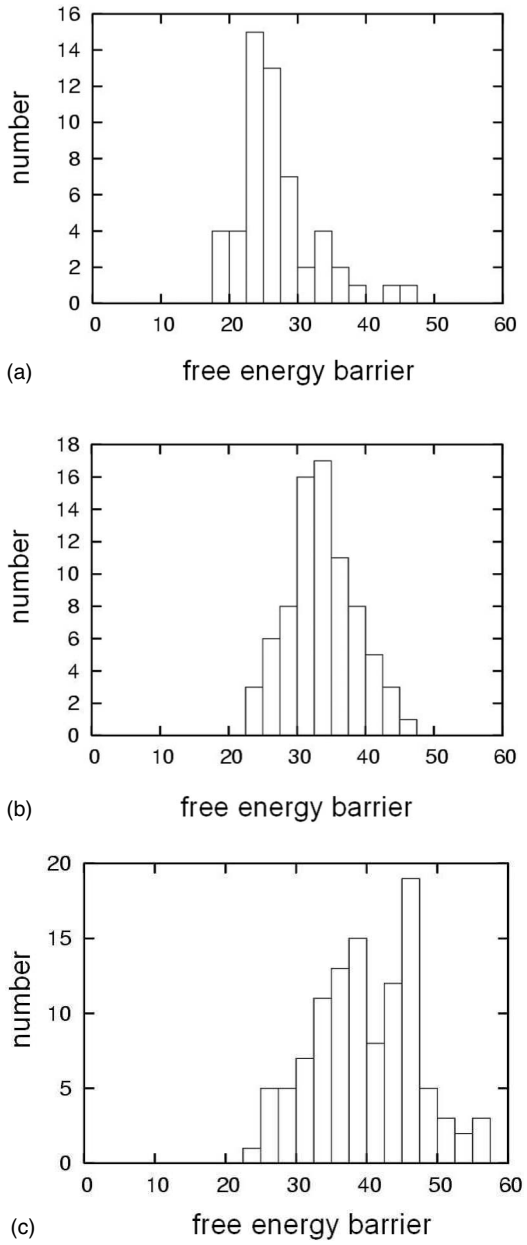

FIG. 4. The histogram of the free-energy barrier for a particle. (a) $\bar{\rho}\sigma^3=0.9$, (b) $\bar{\rho}\sigma^3=0.963$, and (c) $\bar{\rho}\sigma^3=1.06$. The parameter α is set to $\alpha\sigma^2=36$.

using the thermodynamic potential of density functional theory. It has been shown that the behavior of glass-forming systems near T_g can be determined by the waiting-time distribution from the jump motion among basins [15–19]. The distribution of the free-energy barrier can generally be related to the waiting-time distribution [17]. One can thus determine T_g and obtain the thermodynamic and dynamic properties around T_g from the waiting-time distribution [12]. Therefore, the present procedure will open up a different direction of investigation of the glass transition.

As the first application, we have studied the hard-sphere fluid. For the sake of visual presentation, we have constructed the FEL for a tagged particle. The FEL has several basins in addition to the initial basin. These basins are separated by the free-energy barrier which is $(30-60)k_BT$. Such a high barrier may be due to the method to displace the tagged particle. In the present calculation of the free-energy landscape, we forced a displacement of the tagged particle in a particular direction. In the actual system, however, such a displacement may not occur. Since the tagged particle in the confined area is forced to displace in a particular direction, the steric crash which does not occur in the actual system may lead to the high free-energy barrier.

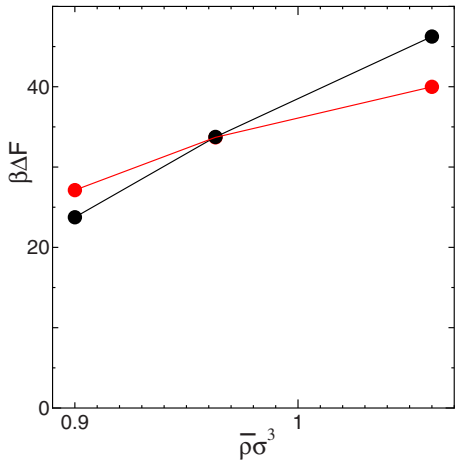

FIG. 5. (Color online) The density dependence of the average free-energy barrier shown in gray (red) and most provable value of the free-energy barrier (black).

We have also obtained the distribution of the free-energy barrier and shown that the density dependence of the most provable value of the barrier and the size of the CRR are nicely correlated. This result supports the basic assumption of the Adam-Gibbs theory [45]. It has not succeeded in obtaining such a result from the experiment and simulation.

In principle, it is possible to analyze the FEL in the entire configurational space of the CRR and obtain the statistics of the FEL. In addition, the present method can also be applied to systems such as colloids and granular materials, which

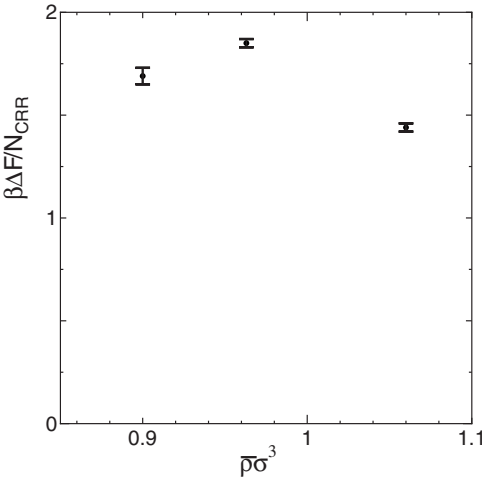

FIG. 6. The density dependence of the ratio $\beta\Delta F/N_{\mathrm{CRR}}$ using the most provable value of the barrier. The weak dependence of this plot supports the Adam-Gibbs theory.

exhibit a jamming transition [46]. As shown by Odagaki [17], however, the waiting-time distribution for the jump motion among basins does not depend on the detail of the barrier structure and is expected to obey a power-law function.

In the present study, we have treated α as a constant for simplicity. It is necessary to incorporate the temperature and density dependence of α for a quantitative analysis of the glass transition in the future. One method is to take α from the Debye-Waller factor calculated by the mode-coupling theory [5]. Since the Debye-Waller factor is related to the root-mean-square displacement (RMSD) and the RMSD corresponds to $\sigma/\sqrt{\alpha}$, an equation for determining α can be derived. Thus, the temperature and density dependence of α is obtained from the equation.

The present results do not depend on the initial configuration within the present density range, though Widmer-Cooper *et al.* suggested that the CRR dynamics depends on the initial configuration in the deeply supercooled liquid state [47]. This is because we have treated densities which do not correspond to the deeply supercooled liquid state. The densities we have studied are near the melting density, 0.96 [30], and are much lower than the Kauzmann density, 1.30 [13]. It is a future problem to study the initial configuration dependence of the present result in the deeply supercooled liquid state.

In conclusion, we mention the shape of the CRR assumed. In this paper, we have used a spherical area as the CRR. Another shape like an ellipsoid can be used instead. The particles involved in the relaxation from one basin to an adjacent basin have been shown to make a string motion [13], and these motions may depend on the shape of the confining area. However, we confirmed that the particles adjacent to the confining area hardly displace and, thus, the particles away from the edge of the confining area determine the distribution of the free-energy barrier. Thus, the distribution of the free-energy barrier does not depend strongly on the shape of the CRR, unless particles of the size of the CRR are confined in a shape such as an ellipsoid with a large aspect ratio.

Since the particles at the edge of the confining area hardly displace, the actual size of the CRR may be equal to or less than that estimated in the previous paper [13]. In order to obtain the actual size more accurately, we need to investigate whether the structural relaxation occurs or not when each particle at the edge of the confining area is fixed. This is a problem to be solved in future studies.

ACKNOWLEDGMENTS

This work was supported in part by a Grant-in-Aid for Scientific Research from the Ministry of Education, Culture, Sports, Science and Technology of Japan.

[1] G. E. Gibson and W. F. Giauque, J. Am. Chem. Soc. **40**, 93 (1923).
[2] M. Sugisaki, K. Adachi, H. Suga, and S. Seki, Bull. Chem. Soc. Jpn. **41**, 593 (1968).
[3] H. Vogel, Phys. Z. **22**, 645 (1921).
[4] G. S. Fulcher, J. Am. Ceram. Soc. **8**, 339 (1925).
[5] W. Götze, in *Liquids, Freezing and Glass Transition*, edited by J. P. Hansen *et al.* (North-Holland, Amsterdam, 1989), p. 287.
[6] M. Mézard and G. Parisi, J. Chem. Phys. **111**, 1076 (1999).
[7] M. Goldstein, J. Chem. Phys. **51**, 3728 (1969).
[8] F. H. Stillinger, Science **267**, 1935 (1995).
[9] D. J. Wales, *Energy Landscapes* (Cambridge University Press, Cambridge, England, 2004).
[10] F. Sciortino, J. Stat. Mech.: Theory Exp. (2005) P05015.
[11] T. Yoshidome, A. Yoshimori, and T. Odagaki, J. Phys. Soc. Jpn. **75**, 0504005 (2006).
[12] T. Odagaki, T. Yoshidome, A. Koyama, and A. Yoshimori, J. Non-Cryst. Solids **352**, 4843 (2006).
[13] T. Yoshidome, A. Yoshimori, and T. Odagaki, Phys. Rev. E **76**, 021506 (2007).
[14] T. Odagaki and T. Ekimoto, J. Non-Cryst. Solids **353**, 3928 (2007).
[15] T. Odagaki and Y. Hiwatari, Phys. Rev. A **41**, 929 (1990).
[16] T. Odagaki, J. Matsui, and Y. Hiwatari, Phys. Rev. E **49**, 3150 (1994).
[17] T. Odagaki, Phys. Rev. Lett. **75**, 3701 (1995).
[18] T. Odagaki, Prog. Theor. Phys. Suppl. **126**, 9 (1997).
[19] M. Higuchi and T. Odagaki, J. Phys. Soc. Jpn. **66**, 3134 (1997).
[20] T. Tao, A. Yoshimori, and T. Odagaki, Phys. Rev. E **64**, 046112 (2001).
[21] T. Tao, A. Yoshimori, and T. Odagaki, Phys. Rev. E **66**, 041103 (2002).
[22] T. Odagaki, T. Tao, and A. Yoshimori, J. Non-Cryst. Solids **307-310**, 407 (2002).
[23] T. Odagaki, T. Yoshidome, T. Tao, and A. Yoshimori, J. Chem. Phys. **117**, 10151 (2002).
[24] T. Tao, T. Odagaki, and A. Yoshimori, J. Chem. Phys. **122**, 044505 (2005).
[25] G. Diezemann, J. Chem. Phys. **123**, 204510 (2005).
[26] G. Diezemann and R. Bohmer, J. Chem. Phys. **124**, 214507 (2006).
[27] D. Oxtoby, in *Liquids, Freezing and Glass Transition*, edited by J. P. Hansen *et al.* (North-Holland, Amsterdam, 1989), p. 145.
[28] Y. Singh, Phys. Rep. **207**, 351 (1992).
[29] T. V. Ramakrishnan and M. Yussouff, Phys. Rev. B **19**, 2775 (1979).
[30] J. L. Barrat, J. P. Hansen, G. Pastore, and E. W. Waisman, J. Chem. Phys. **86**, 6360 (1987).
[31] Y. Singh, J. P. Stoessel, and P. G. Wolynes, Phys. Rev. Lett. **54**, 1059 (1985).
[32] C. Dasgupta and O. T. Valls, Phys. Rev. E **58**, 801 (1998).
[33] C. Dasgupta and O. T. Valls, Phys. Rev. E **59**, 3123 (1999).
[34] X. Xia and P. G. Wolynes, Proc. Natl. Acad. Sci. U.S.A. **97**, 2990 (2000).
[35] C. Kaur and S. P. Das, Phys. Rev. Lett. **86**, 2062 (2001).
[36] C. Kaur and S. P. Das, J. Phys.: Condens. Matter **13**, 7259

(2001).
[37] K. Kim and T. Munakata, Phys. Rev. E **68**, 021502 (2003).
[38] S. P. Singh and S. P. Das, J. Non-Cryst. Solids **352**, 4857 (2006).
[39] S. P. Singh and S. P. Das, J. Phys.: Condens. Matter **19**, 246107 (2007).
[40] J. P. Hansen and L. R. Mcdonald, *Theory of Simple Liquids* (Academic, London, 1986).
[41] W. A. Curtin and N. W. Ashcroft, Phys. Rev. A **32**, 2909 (1985).
[42] A. R. Denton and N. W. Ashcroft, Phys. Rev. A **39**, 4701 (1989).
[43] Y. Rosenfeld, Phys. Rev. Lett. **63**, 980 (1989).
[44] The relative error can be estimated as follows. We first define the free-energy barrier and that for a particle as F and $f \equiv F/N_{\mathrm{CRR}}$, respectively. Since the FEL is obtained by displacing the tagged particle and relaxing other particles, the difference from the saddle point, ΔF, can be expressed as $\Delta(N_{\mathrm{CRR}} f) \sim \Delta N_{\mathrm{CRR}} \Delta f \sim \Delta f$. Therefore, the relative error is given by $1/N_{\mathrm{CRR}}$, which is of the order of a few percent.
[45] G. Adam and J. H. Gibbs, J. Chem. Phys. **43**, 139 (1965).
[46] A. J. Liu and S. R. Nagel, Nature (London) **396**, 21 (1998).
[47] A. Widmer-Cooper, P. Harrowell, and H. Fynewever, Phys. Rev. Lett. **93**, 135701 (2004).